

Imaging of the Thyroid

Practical Approach



Susana Calle, MD^{a,*}, Jeanie Choi, MD^b, Salmaan Ahmed, MD^a, Diana Bell, MD^c, Kim O. Learned, MD^a

KEYWORDS

• Thyroid • Imaging • Benign • Malignant • Cross-sectional • Ultrasound

KEY POINTS

- Ultrasound examination is a cost-effective modality for diagnostic purposes and biopsy guidance in thyroid disease. Computed tomography is the workhorse for thyroid tumor staging. Radionuclide scintigraphy evaluates thyroid function.
- Thyroid imaging features can be classified as either diffuse or focal.
- Diffuse multinodular goiter and thyroiditis are common benign conditions. Focal nodules should be evaluated sonographically for benign and malignant features using Thyroid Imaging and Data System guidelines.
- Imaging detection of local invasiveness of a thyroid lesion and nodal metastasis may lead to expedient diagnosis of aggressive thyroid malignancy.
- Key imaging features suspicious for malignancy in a background of diffuse benign disease include focal highly suspicious hypoechoic nodule, microcalcifications, asymmetric lobar involvement and focal fluoro-2-deoxy-D-glucose avidity.

INTRODUCTION

The thyroid gland plays a critical role in regulating metabolic functions and imaging has long been established as an essential element in the workup of abnormal thyroid function and clinically suspected lesions of the thyroid gland. Knowledge of the imaging modalities as well as normal and abnormal imaging appearances of the thyroid gland and pathologies is essential for appropriate identification and diagnosis of thyroid lesions. In this article, we discuss the pertinent anatomy and nodal drainage and review the imaging appearance of common thyroid diseases, with a special emphasis on a practical imaging approach to expedient diagnosis of highly prevalent thyroid conditions such as Grave's disease, goiter,

thyroiditis, and thyroid cancer. The relative roles of various imaging modalities in the evaluation of various thyroid diseases are included.

ANATOMY

The thyroid gland is a shield-shaped gland located superficially in the infrahyoid neck over the cricoid and trachea (**Fig. 1**). The right and left thyroid lobe join inferiorly by a thin band of tissue over the anterior trachea known as the isthmus. Anteriorly, the thyroid gland abuts the strap musculature and sternocleidomastoid muscles. The carotid arteries and jugular veins are located lateral and posterior to the gland, and the posterior margin of the thyroid abuts the longus coli muscles.¹ An accessory, pyramidal lobe, is present in approximately 50% to

The authors have no pertinent commercial or financial conflicts of interest to disclose.

^a Department of Neuroradiology, Division of Diagnostic Imaging, The University of Texas MD Anderson Cancer Center, 1400 Pressler Street Unit 1482, Houston, TX 77030, USA; ^b Neuroradiology Section, Department of Diagnostic and Interventional Imaging, The University of Texas Health Science Center at Houston, 6431 Fannin Street, Houston, TX 77030, USA; ^c Head and Neck Section, Departments of Pathology and Head and Neck Surgery, The University of Texas MD Anderson Cancer Center, 1515 Holcombe Boulevard, Houston, TX 77030, USA

* Corresponding author.

E-mail address: susanacalle@gmail.com

Neuroimag Clin N Am 31 (2021) 265–284

<https://doi.org/10.1016/j.nic.2021.04.008>

1052-5149/21/© 2021 Elsevier Inc. All rights reserved.

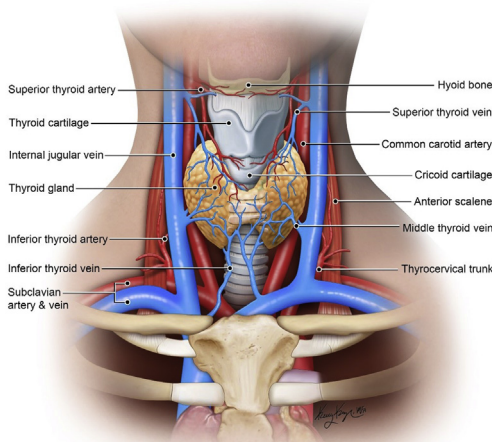


Fig. 1. Illustration of the thyroid gland and anatomic landmarks. (Courtesy of Kelly Kage, MFA, CMI, Houston, TX.)

70% of the population and arises from the isthmus and extends superiorly along the course of the distal thyroglossal duct.²

A thin fibrous capsule surrounds the thyroid gland with septated projections that extend into the thyroid parenchyma to divide thyroid tissue into lobules. A rich vascular network is supplied by paired superior and inferior thyroidal arteries, which are branches of the external carotid arteries and thyrocervical trunks, respectively. The thyroid gland receives innervation from the vagus nerve and the cervical sympathetic plexus, which influence gland perfusion.²

Lymphatic drainage of the gland includes the deep lateral cervical nodal levels I to V, the central anterior nodal levels VI to VII (prelaryngeal/Delphian, pretracheal, paratracheal, and superior mediastinum) and retropharyngeal nodal groups. Although the inferior portions of the gland and the isthmus tend to drain to the paratracheal and lower deep cervical level III to IV nodes, the superior gland drains into the superior pretracheal, prelaryngeal/Delphian, and level II to III cervical groups, explaining the propensity of skip metastasis to the upper nodal group in tumors arising from the upper pole of the thyroid.³

For the specific purpose of multidisciplinary agreement in staging and management of thyroid carcinoma, the American Joint Committee on Cancer and the American Thyroid Association (ATA) use the classic I to VI cervical nodal stations to describe pertinent nodal disease^{4,5} (Fig. 2). The benefits of the nodal classification method are reproducible consistency mapping with the limits of the compartments readily identified on imaging, clear surgical correlates, and consensus

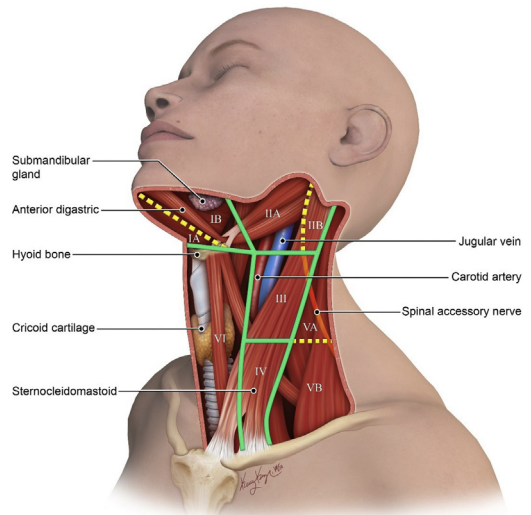


Fig. 2. Illustration of the nodal compartments of the neck. (Courtesy of Kelly Kage, MFA, CMI, Houston, TX.)

communication across specialties. Thyroid cancer nodal staging is defined by central anterior compartment (level VI and VII), or lateral compartment (levels I–V) and retropharyngeal nodal metastasis, and is detailed in an article in this series, titled *Imaging of Cervical Lymph Nodes in Thyroid Cancer: Ultrasound and Computed Tomography* by Chasen and colleagues.

IMAGING FINDINGS

Ultrasound Imaging

Ultrasound examination constitutes the most sensitive imaging modality in the evaluation of the thyroid gland. Added benefits include availability, low cost, and lack of ionizing radiation.¹ Real-time ultrasound examination performed with high-resolution linear array transducers ranging from 7.5 to 12.0 MHz provides detailed evaluation of focal and diffuse thyroid disease and assessment of cervical nodes. Additionally, ultrasound examination is essential in guiding fine-needle aspiration procedures for histopathologic diagnosis.

The normal appearance of the thyroid gland on ultrasound examination is that of a well-defined homogeneous gland, which is hyperechoic relative to adjacent musculature and is draped along the anterior trachea.¹ On average, the thyroid isthmus measures 3 mm in thickness and each lobe measures 4 to 6 cm in length and up to 2 cm in both transverse and anteroposterior dimensions.¹

Cross-sectional Imaging

Cross-sectional imaging modalities, including computed tomography (CT) scans and MR

imaging of the neck, are an important adjunct in the evaluation of patients with thyroid disease, and obtained from the level of the tracheal bifurcation inferiorly to the skull base superiorly. These techniques allow for the interrogation of disease extent and nodal stations not readily accessible to ultrasound examination, including the lateral retropharyngeal compartments and retrosternal upper mediastinum. Furthermore, cross-sectional imaging allows for the characterization of tumor invasion into deep and neighboring structures, which upstages thyroid malignancies.² Gross extrathyroidal extension (ETE) to the strap muscles will upstage to T3b disease, regardless of tumor size for thyroid cancer.⁵ The invasion of tissue beyond the strap muscles, including subcutaneous soft tissues, larynx, trachea, esophagus, and recurrent laryngeal nerve, would classify the primary tumor as T4a and extension to the prevertebral fascia or encasement of carotid or mediastinal vessels as T4b.⁵ The commonly encountered thyroid cancers and discussion of changes in staging in the most recent American Joint Committee on Cancer, eighth edition, will be highlighted in malignant thyroid disease section elsewhere in this article.

On CT imaging, owing to the iodine content of the thyroid, the gland is intrinsically hyperdense on noncontrast imaging with Hounsfield units ranging from 80 to 100. Iodinated contrast administration is recommended for better evaluation of the gland, which shows avid homogenous enhancement, the surrounding structures, and cervical nodes.⁶ Iodine is generally cleared within 4 to 8 weeks in most patients, so concern about iodine burden from intravenous contrast causing a clinically significant delay in subsequent whole-body radioactive iodine scan or radioactive iodine ablation treatment after the contrast CT imaging followed by surgery is generally unfounded.⁴

MR imaging allows for improved soft tissue differentiation, whereas CT scans have greater spatial resolution and remains the imaging workhorse.⁷ The neck MR imaging generally includes a T1-weighted image, T2-weighted sequence, fat-saturated T2-weighted sequence, followed by postcontrast fat-saturated T1-weighted images. The normal appearance of the thyroid gland is that of a homogeneous, smoothly marginated parenchyma that is, isointense on T1, slightly hyperintense on T2, and demonstrates homogeneous enhancement compared with adjacent muscle.⁷

The soft tissue differentiation provided by MR imaging allows for the characterization of diffuse and focal thyroid disease. Findings of diffuse thyroid disease include variations in size, signal intensity, enhancement degree and pattern, and margin

contour.⁷ Furthermore, studies have explored the diagnostic potentials of MR imaging, including diffusion-weighted imaging, T2 signal intensity, and dynamic contrast-enhanced parameters, for the characterization of benign and malignant thyroid nodules.⁸ In 1 study, the T2 signal intensity ratio is calculated by measuring the mean signal intensity of the nodule divided by the signal intensity of the paraspinal muscle, and both the T2 signal intensity ratio and the apparent diffusion coefficient values in papillary thyroid carcinoma (PTC) were significantly lower than for benign nodules.⁸⁻¹⁰ These studies offer promising results in the classification of thyroid nodules, but the heterogeneity of diffusion and perfusion techniques, time consuming and cumbersome postprocessing, and higher cost hinder their widespread application and validation at this time.

Nuclear Medicine

Radionuclide imaging has been available for many years and allows for excellent functional evaluation of the thyroid gland. The most frequently used radiotracers in thyroid scintigraphy include technetium-99m pertechnetate and iodine-based tracers, including ¹²³I and ¹³¹I. Additionally, gallium-67 may be used in the evaluation of thyroid lymphoma.

Scintigraphic imaging with I¹²³ is valuable in the characterization of thyroid nodules as either “hot” or “cold,” depending on whether there is focal radiotracer accumulation or a focal photopenic defect, respectively.¹¹ Cold thyroid nodules have a greater incidence of malignancy, calculated at 10% to 20%, and therefore require further evaluation with possible biopsy. Conversely, hot nodules in the setting of low thyroid-stimulating hormone, are generally benign and may not require further studies.¹¹ ¹³¹I is beneficial in the acquisition of whole body imaging following thyroidectomy and thyroid ablation for the detection of residual tissue and metastatic disease.¹¹

The normal thyroid gland on PET imaging using 2-[fluorine-18] fluoro-2-deoxy-D-glucose (FDG) shows homogeneous radiotracer uptake similar to that of adjacent muscle.¹¹ PET-CT scanning relies on high glucose metabolism and therefore increased tracer uptake will generally be greater in cases of poor tumor differentiation with a greater risk of metastatic disease. For this reason, PET is generally used in high-risk patients and is not routinely recommended for determining disease extent in low-risk populations.¹²

It has been estimated that approximately 2% to 3% of PET imaging reveals an incidental thyroid nodule. Although higher standardized uptake

value measurements have been documented in malignant versus in benign nodules, no specific threshold has been defined to predict malignancy. However, increased uptake has been associated with a 14% to 40% greater increase in risk of malignancy and should therefore prompt further evaluation with ultrasound examination and ultrasound-guided biopsy if pertinent.¹¹ The management of FDG-avid nodules on PET/CT is further addressed in the article of this series, titled *PET/Computed Tomography in Thyroid Cancer* by Yadav and colleagues.

PRACTICAL APPROACH TO IMAGING EVALUATION

When confronted with thyroid disorders, it is beneficial to establish a basic mental framework that

will allow the radiologist to categorize the entity in a broad fashion (**Fig. 3**). First, imaging features of the thyroid gland can be classified as either diffuse or focal. Diffuse abnormality of the thyroid gland must prompt the radiologist to consider multinodular goiter and the spectrum of thyroiditis, which are generally benign conditions. However, it is important to recognize instances where diffuse infiltration of the gland may signify malignant pathology, such as with the diffuse sclerosing variant of PTC, and keen attention to detect malignancy within the diffuse benign disease, such as the development of PTC and/or lymphoma in the setting of Hashimoto thyroiditis and diffuse metastatic infiltration of the thyroid gland.

Conversely, focal lesions and each nodule in the multinodular goiter should be evaluated for benign or malignant features to determine management.

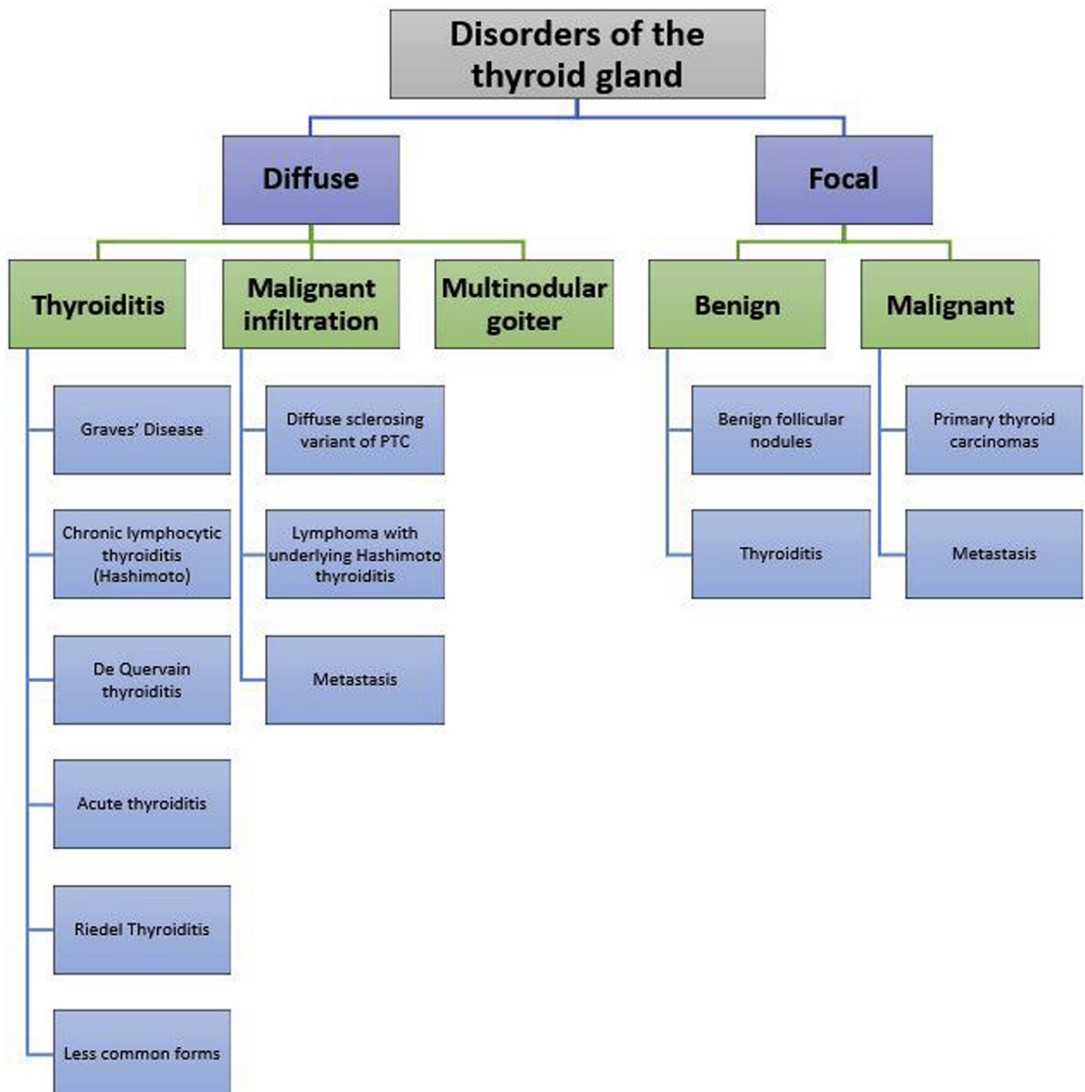


Fig. 3. General approach to classification of disorders of the thyroid gland.

The implementation of the Thyroid Imaging and Data System (TI-RADS) and ATA guidelines aid in determining the risk of malignancy and the subsequent management strategies for thyroid nodules based on imaging features pertaining to nodule composition, echotexture, and shape, among other features. The assessment and classification of thyroid nodules will be addressed in detail in the article of this series, titled [Ultrasound of Thyroid Nodules and the Thyroid Imaging Reporting and Data System](#) by Harshawn Malhi and Edward Grant.

The thorough exploration of cervical nodes serves as an important adjunct in the diagnosis of thyroid pathology. The presence of unilateral versus bilateral adenopathy has different implications as does size, echogenicity, morphology, and vascularity. Normal and reactive nodes tend to be oval shaped and slightly hypoechoic to muscle with central echogenic hila and organized flow on Doppler imaging.¹³ In contrast, thyroid nodal metastases will display cystic transformation, internal calcifications, or hyperechogenic foci with 100% specificity and positive predictive value as well as less specific suspicious findings of rounded morphology and disorganized vascular flow.^{13,14} The article of this series, titled [Imaging of Cervical Lymph Nodes in Thyroid Cancer: Ultrasound and Computed Tomography](#) by Chasen and colleagues, goes into greater detail regarding benign and malignant nodal imaging features.

Furthermore, attention to key points pertaining to clinical presentation may also help narrow down differential considerations further. For instance, a nontender goiter and hypothyroidism in the setting of diffuse thyroid infiltration may alert to Hashimoto thyroiditis. Conversely, a painful transient thyrotoxic state with suppressed thyroid-stimulating hormone can indicate subacute thyroiditis.¹⁵ Similarly, a rapidly progressing thyroid mass with imaging signs of ETE should raise suspicion for anaplastic thyroid carcinoma. These clues pertaining to the patient's symptomatology, among others, are essential in guiding diagnosis and therapy.

BENIGN THYROID DISEASE

Graves' Disease

Graves' disease is an autoimmune condition wherein autoantibodies are produced against thyroid proteins, most notably to the thyroid-stimulating hormone receptor.¹⁶ The resultant effects include hyperplasia of the thyroid with accompanying autonomous function of the gland and hyperthyroidism with elevated free T3 and T4 levels in the setting of decreased serum thyroid-stimulating hormone. This

entity is more common in females between the ages of 20 and 50 years.¹⁶ The clinical presentation is characterized by a triad consisting of hypertrophy of the thyroid gland, exophthalmos secondary to infiltrative ophthalmopathy, and pretibial myxedema. Although the basis of diagnosis lies in the clinical and laboratory features of the disease, imaging with ultrasound and Doppler imaging of all hyperthyroid patients is generally widely recommended.^{16,17}

Ultrasound features include diffuse enlargement of the gland, including the thyroid isthmus, with a rounded contour and variable echotexture. The gland may seem to be diffusely hypoechoic and heterogeneous or alternatively may be normal in echotexture. Exploration with Doppler imaging reveals a characteristically diffuse increase in parenchymal vascularity, termed "thyroid inferno" ([Fig. 4](#)). Of note, the degree of increased vascularity does not correlate directly with the level of hyperthyroidism and generally reflects inflammatory changes in the gland.¹⁶

Thyroid scintigraphy reveals diffuse enlargement of the gland with homogeneous elevation of radiotracer uptake at 24 hours relative to background activity owing to both increased function and increased stimulation.¹⁸ The increased activity may result in the visualization of the pyramidal lobe that, owing to its small size, is not typically identified (see [Fig. 4](#)).¹⁸

Cross-sectional imaging with a CT scan and MR imaging is not generally recommended as a workup for presumptive Graves' disease. Findings are generally nonspecific revealing an enlarged gland with decreased Hounsfield units on CT imaging and avid enhancement and increase T1 and T2 signal intensity on MR imaging owing to parenchymal and vascularity changes.¹⁹

Thyroiditis

Thyroiditis, representing inflammation of the thyroid gland, generally manifests as diffuse heterogeneous echotexture on ultrasound with heterogeneous attenuation on CT imaging ([Fig. 5](#)). Exploration with Doppler imaging may additionally demonstrate widespread increased vascularity.¹¹ The entity can be subclassified as chronic lymphocytic thyroiditis, de Quervain thyroiditis, acute thyroiditis, Riedel thyroiditis, or other less common forms.¹¹ Chronic lymphocytic thyroiditis, also known as Hashimoto thyroiditis, is an autoimmune disorder and the most common cause of hypothyroidism in the United States. Histologically, this form of thyroiditis demonstrates a combination of inflammatory cells and Hurthle cells. Specifically, for Hashimoto thyroiditis to be diagnosed, specific

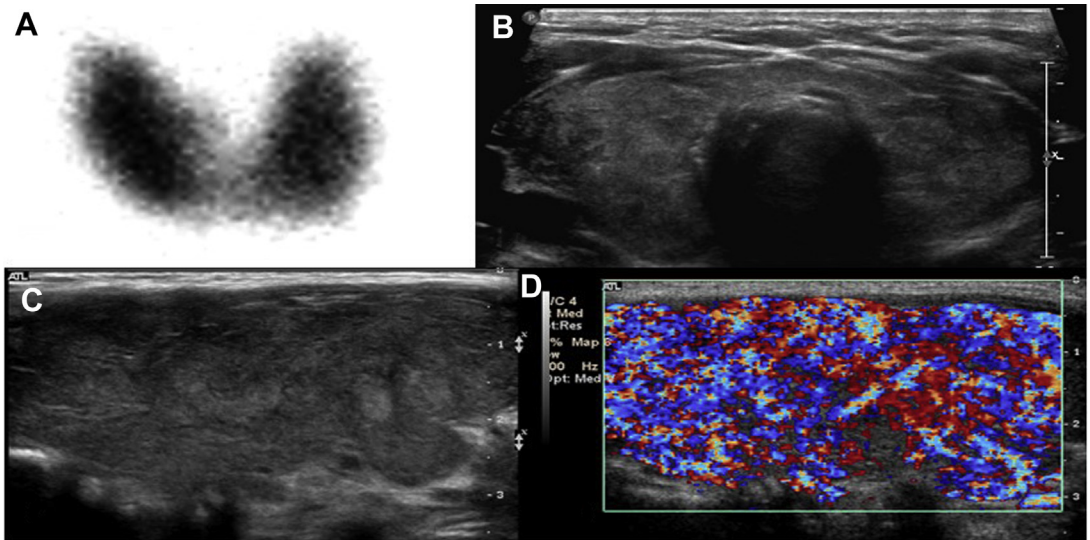


Fig. 4. Graves' disease. Thyroid scintigraphy (A) reveals diffuse thyroid enlargement with homogeneous increase in thyroid uptake at 24 hours. Transverse midline (B) and longitudinal view of the right thyroid lobe (C) grayscale ultrasound examination shows increased size of the thyroid gland, with rounded contours and heterogeneous echotexture. Exploration with color Doppler imaging (D) of the right thyroid lobe shows markedly increased parenchymal vascularity, termed "thyroid inferno."

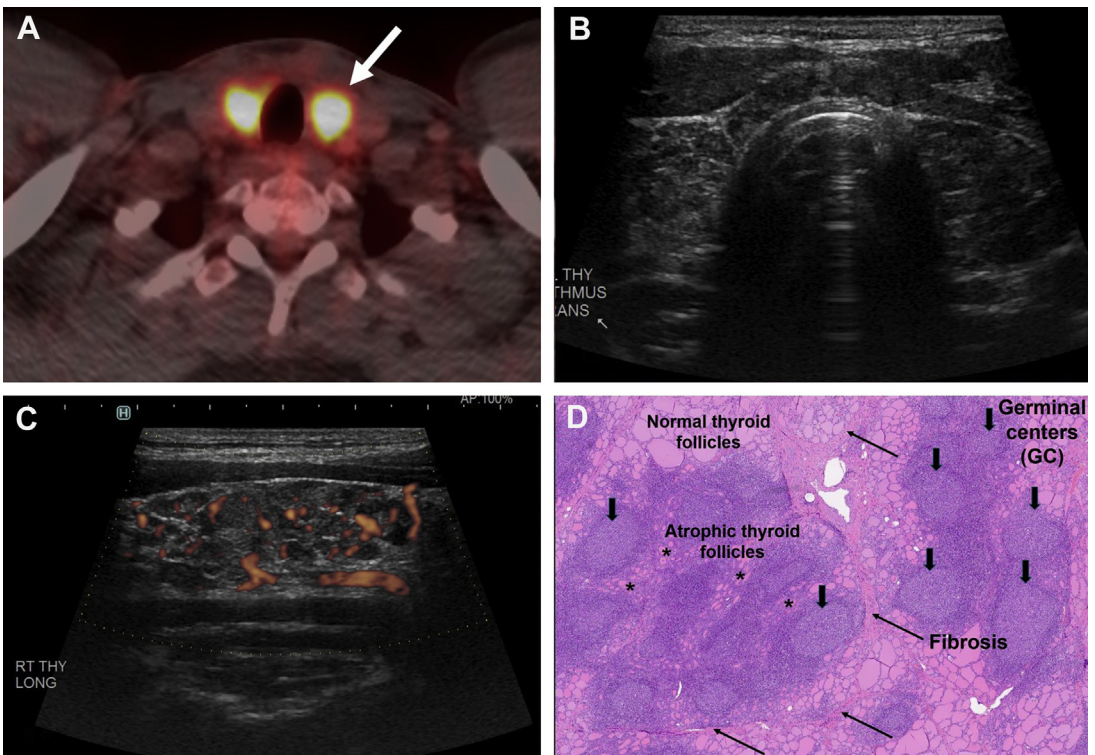


Fig. 5. Hashimoto thyroiditis. Axial fused FDG PET/CT image (A) shows diffusely increased FDG uptake with standardized uptake values of up to 12 (white arrow). Transverse midline (B) grayscale ultrasound imaging reveals heterogeneous echotexture owing to a confluence of small hyperechoic nodules and micronodules with diffusely increased vascularity on power Doppler imaging (C). Histologic examination of tissue sample with hematoxylin and eosin staining (D) shows a combination of both normal and atrophic thyroid follicles, fibrosis and germinal centers.

antithyroid peroxidase and antithyroglobulin antibodies must be detected.

A common ultrasound appearance of Hashimoto thyroiditis is the heterogeneous echotexture of the thyroid parenchyma characterized by multiple hypoechoic micronodules (see **Fig. 5**). In Hashimoto thyroiditis, micronodulation corresponds to accentuated thyroid lobulation on the pathologic specimen. The reported positive predictive value for micronodulation in diagnosing Hashimoto thyroiditis was 94.7%. Sonographically, micronodules are generally 0.1 to 0.65 cm in size, hypoechoic, and surrounded by an echogenic rim. The hypoechogenicity of micronodules is due to massive infiltration by an exudate of lymphocytes and plasma cells similar to the hypoechogenicity caused by lymphoma. Formation of fibrous strands around the lobules causes a hyperechoic ring around each micronodule. The majority of micronodules, however, do not grow beyond 0.6 cm in size, distinguishing them from the larger hypoechoic lymphoma.²⁰ Ultrasound patterns associated with a 100% specificity for benignity include a “giraffe pattern” and the “white knight pattern,” which are associated with Hashimoto thyroiditis.²¹ The original giraffe pattern described by Bonavita is composed of thin hypoechoic septations surrounding rounded hyperechoic foci giving the lesion the appearance of giraffe fur (**Fig. 6**).²² The white knight is a term given to a homogeneously hyperechoic nodule (**Fig. 7**). Correct identification of these patterns precludes the need for histologic confirmation.

The proposed association between Hashimoto thyroiditis and PTC remains a controversial topic. The frequent coexistence of these 2 entities suggests an underlying relationship. The prevalence of PTC in the setting of underlying Hashimoto

thyroiditis is also greater than that in the general population. In patients who had undergone total thyroidectomy with a preoperative diagnosis of Hashimoto thyroiditis, the incidence of PTC was calculated at 40.2% for nodular variant Hashimoto thyroiditis and 8.1% for diffuse variant Hashimoto thyroiditis.²³ Conversely, in patients undergoing thyroidectomy for normofunctioning goiter, the incidence of PTC was reported at 7.7%.²³ The detection of focal hypoechoic nodule larger than the 0.6 cm size of micronodules in Hashimoto thyroiditis, clustered microcalcifications, or dystrophic calcification with asymmetric lobar involvement should prompt the radiologist to suspect PTC in the setting of underlying Hashimoto thyroiditis (**Fig. 8**). Furthermore, special attention must be paid to thorough assessment of cervical nodes for the detection of lateral cystic lymphadenopathy.

An additional association exists between Hashimoto thyroiditis and the development of primary thyroid lymphoma (PTL). Data suggesting their correlation include a greater reported incidence rate of PTL in patients with Hashimoto thyroiditis, reported at 16 persons per year per 10,000 persons, significantly higher than that of the general population, with some studies suggesting a 60-fold higher risk.²⁴ Furthermore, antithyroid peroxidase antibodies have been detected in approximately 60% to 80% of patients with PTL, which further indicates Hashimoto thyroiditis as a risk factor for the development of PTL.²⁴ It is suggested that the presence of lymphocytes in Hashimoto thyroiditis that undergo chronic antigenic stimulation predisposes them to malignant transformation.²⁴ On ultrasound examination, diffuse asymmetric enlargement of

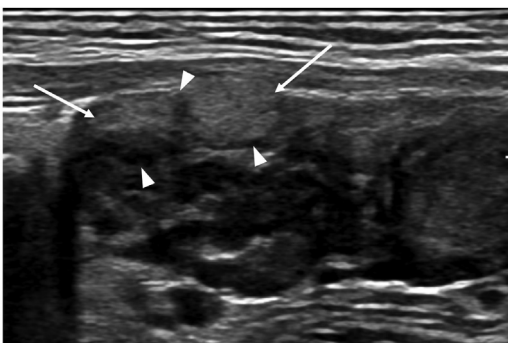


Fig. 6. Hashimoto thyroiditis. Longitudinal grayscale ultrasound of the thyroid parenchyma demonstrates a focal area with a giraffe pattern characterized by hyperechoic nodules (arrows) separated by hypoechoic septations (arrowhead).



Fig. 7. Hashimoto thyroiditis. Longitudinal gray-scale ultrasound image of the right thyroid lobe shows homogeneously hyperechoic nodule termed the white knight (arrow) on a background of a diffusely heterogeneous parenchymal echotexture.

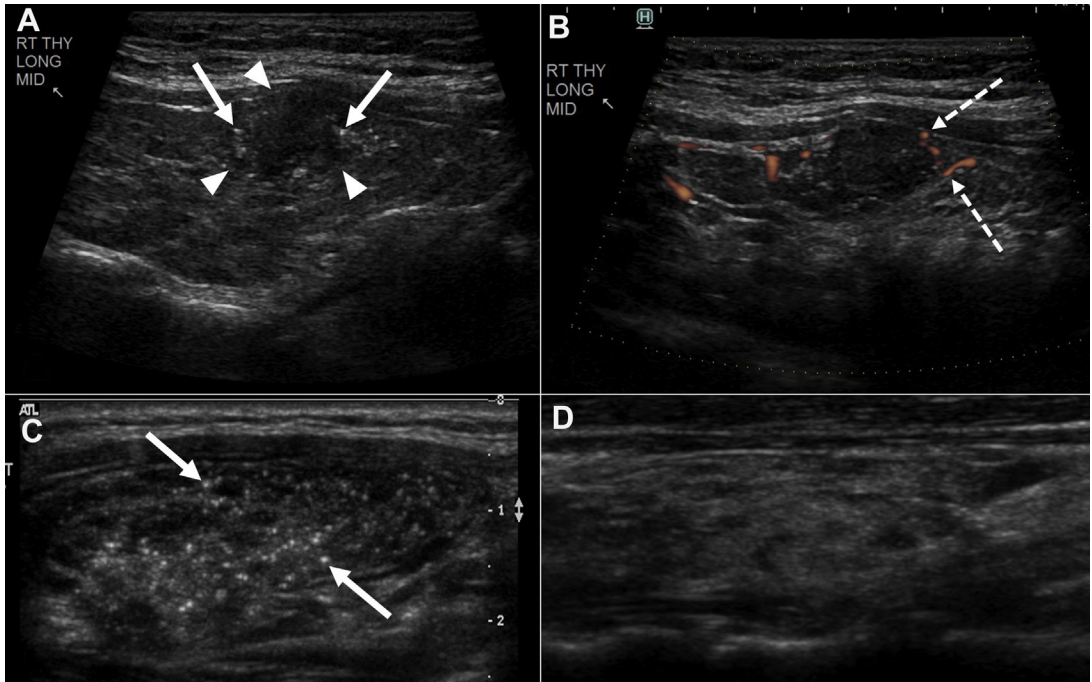


Fig. 8. Hashimoto thyroiditis and PTC. A grayscale ultrasound longitudinal view (A) of the right thyroid lobe shows a focal confluent 1.5 cm hypoechoic nodule standing out from the background of thyroiditis (*arrowheads*) with irregular borders, internal microcalcifications (*white arrows*), and mild peripheral vascularity (*dashed arrows*) on power Doppler imaging (B) consistent with biopsy-proven PTC. A grayscale ultrasound longitudinal view of the right lobe (C) and left lobe (D) in a different patient illustrate the diffuse hypoechoic PTC with microcalcifications (*arrows*) infiltrating the entire right lobe, in contrast with the benign heterogeneous hyperechoic Hashimoto thyroiditis of the left lobe.

the gland with homogeneously hypoechoic, lobulated contour and increase through transmission are features of PTL in underlying Hashimoto thyroiditis (**Fig. 9**).

Multinodular Goiter

Whenever facing a diffuse multinodular thyroid, it is comforting to know that an estimated 60% to 70% of thyroid nodules in which fine needle aspiration is performed are classified as benign.¹¹

The majority of these represent either benign follicular nodules or thyroiditis. Benign follicular nodules comprise a range of nodules including nodular goiter, adenomatoid or hyperplastic nodules, colloid nodules, nodules of Grave's disease, and follicular adenomas, which are composed of varying proportions of benign follicular cells and colloid material on histology.¹¹ However, the incidence of thyroid cancer in multinodular goiter is the same and one must search for high suspicious features of the nodules as demonstrated by ATA



Fig. 9. Thyroid lymphoma in Hashimoto thyroiditis. Transverse (A) and longitudinal (B) view grayscale ultrasound images of the right thyroid lobe shows a 3-cm lobulated, diffusely hypoechoic nodule (*white arrows*) with increase through transmission and internal vascularity (*dashed arrow*) on power Doppler (C). Surgical pathology revealed B-cell lymphoma in Hashimoto thyroiditis (not shown).

and TI-RADS, as well as the detection of cystic or calcific pathologic neck lymph nodes.

Both the giraffe and the white knight patterns, associated with Hashimoto thyroiditis (as detailed in the Thyroiditis section), were previously introduced as ultrasound patterns with a 100% specificity for benignity. Additional patterns that preclude histologic confirmation include spongiform nodules and “cysts with colloid clot” associated with benign follicular nodules.^{19,21} Spongiform nodules are composed of microcystic foci making up a honeycomb pattern.²⁵ A cyst with colloid clot refers to a cystic nodule with an avascular retracted clot with the clot having a similar honeycomb appearance to a spongiform nodule.²² The correct identification of these patterns could obviate more than 60% of biopsies.²²

Cross-sectional imaging, in particular CT scans, can be obtained in patients with a multinodular goiter to determine the extent of mediastinal extension not assessed by ultrasound examination (Fig. 10). This consideration is important in the preoperative evaluation of patients, as demonstrated in 1 series of 665 patients, of whom 9.5% required sternotomy for goiter resection rather than the typical cervical approach.²⁶ Preoperative planning with CT scan or MR imaging can more clearly define factors that would prompt the surgeon for a thoracic approach including size larger than the thoracic inlet, substernal extension or extension to the aortic arch and loss of clear plane of tissue around the goiter in the mediastinum (see Fig. 10).²⁶

MALIGNANT THYROID DISEASE

Considering the vast literature on oncologic thyroid diagnosis and management, it is a daunting

task to provide a comprehensive discussion of thyroid cancer. The assessment of thyroid nodules for malignant features are addressed in detail in the article of this series, titled [Ultrasound of Thyroid Nodules and the Thyroid Imaging Reporting and Data System](#) by Harshawn Malhi and Edward Grant. The following review highlights the commonly encountered thyroid malignancy with key diagnostic features and staging.

Approximately 3% to 7% of biopsied thyroid nodules are malignant with an additional 3% to 5% reported as suspicious for malignancy.¹¹ Primary thyroid cancer is the most common malignancy, of which 80% are PTC, with lymphoma and metastatic disease being less frequent. Thyroid follicular epithelial-derived cancers are divided into 3 major common categories: papillary (differentiated, 85%), follicular (differentiated, 12%), and anaplastic (undifferentiated, <3%). Medullary thyroid carcinoma originates from the neural crest derived parafollicular C-cells of the thyroid gland, distinguishing it as a separate category from follicular cell-derived cancers.

Local invasiveness of a thyroid nodule raises a red flag for thyroid malignancy, both clinically and radiographically, and is more commonly seen in anaplastic thyroid carcinoma, lymphoma, and sarcoma.²⁷ It is suggested clinically by difficulty breathing, voice changes, and dysphagia owing to involvement of the trachea and larynx, recurrent laryngeal nerve, and esophagus, respectively.²⁷ Cross-sectional imaging plays a critical role in delineating adjacent structural invasion, substernal extent of tumor, involvement of mediastinal structures and prevertebral space, and carotid encasement, which define resectability, surgical planning, and the potential need for sternotomy and reconstruction.²⁶ For example, when tumor invasion of

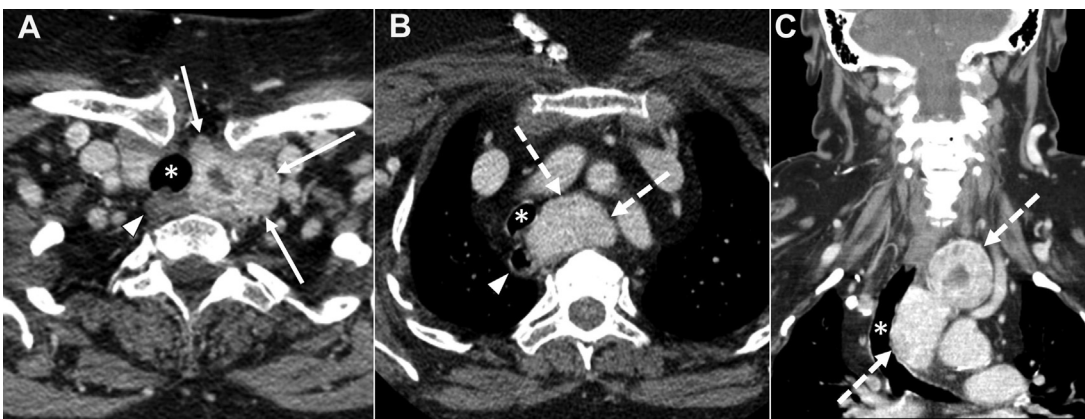


Fig. 10. Multinodular goiter. Axial (A, B) and coronal (C) postcontrast CT images of the neck show an enlarged left-sided thyroid goiter (arrow) with substernal extension into the mediastinum to the aortic arch (dashed arrows). The mediastinal component displaces the trachea (*) and esophagus (arrowhead) to the right.

the trachea extends inferiorly below the level of the sternum, the probability of the need for sternotomy increases.²⁸ Assessment for tracheal and/or esophageal invasion on cross-sectional imaging aids in complete presurgical evaluation to prevent incomplete resection and need for revision surgery.²⁸

On imaging, local invasion is detected by extension of the tumor beyond the confines of the thyroid contour or frank invasion of neighboring structures.²⁷ Strap muscle involvement can be ascertained with increased certainty when the tumor extends through the muscle to the opposing surface (Fig. 11).²⁹ Loss of the echogenic capsule on ultrasound examination is the best predictor of the presence of extracapsular extension (T3b disease) with 75% sensitivity and 65% specificity (Fig. 12). When 3 to 4 features of capsular abutment, contour bulging, loss of echogenic capsule, and vascularity beyond the capsule are present, the specificity increases to 70% to 93% with low sensitivity of 63% to 25% (see Figs. 11 and 12). However, because T3b disease is resectable, the low sensitivity of imaging evaluation for strap muscle invasion may not be significant clinically.³⁰

In the evaluation of tracheal and esophageal invasion, tumor contact of more than 180° with the trachea or esophagus, tracheal deformity, or loss of normal wall of the esophagus, or intraluminal mucosal tumor has high specificity (90%) but low sensitivity (30%–60%) (see Figs. 11 and 12).³¹ The loss of the fat planes in the tracheoesophageal

groove, more than 25% of tumor abutting the capsule at the posterior thyroid and evidence of vocal cord paralysis on CT scan and/or clinical evaluation predict tumor invasion of the recurrent laryngeal nerve when at least 2 of these findings are present (see Fig. 12; Fig. 13).³¹ Deformity of the common carotid artery contour and more than 180° circumferential contact with tumor increases the probability of vascular invasion, with more than 270° circumferential involvement, likely rendering the tumor unresectable.³²

In the recent eighth edition of the American Joint Committee on Cancer staging system for differentiated thyroid cancer, notable changes were made from the seventh edition, resulting in the downstaging of many patients and included increasing the age cutoff for staging from 45 to 55 years (Table 1).³³ Microscopic invasion of tumor into adjacent soft tissues was removed as a component of T3 disease, with T3 disease now divided into T3a (>4 cm isolated to the thyroid) and T3b (any size tumor with gross ETE into strap muscles).³⁴ In patients 55 years of age or older, stage III disease under the eighth edition is now defined as gross invasion into subcutaneous soft tissues and posterolateral structures including the larynx, trachea, recurrent laryngeal nerve and esophagus.³³ Vascular encasement involving the carotid arteries and mediastinal arteries as well as involvement of the prevertebral fascia now define stage IVA disease.

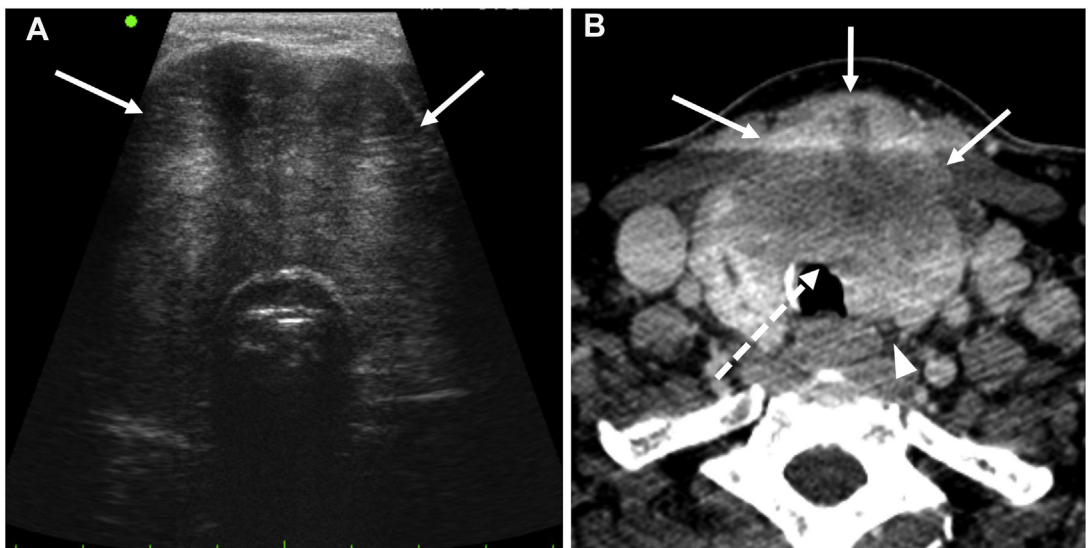


Fig. 11. Invasive PTC. Transverse grayscale ultrasound image of the thyroid gland (A) shows a hypoechoic solid mass infiltrating the isthmus with capsular abutment and contour bulging (arrows). Axial postcontrast CT image of the neck (B) complements findings on ultrasound and delineates anterior ETE of the mass to the strap muscles (arrows) and intraluminal mucosal invasion of the trachea (dashed arrow). Note the preservation of the tracheoesophageal groove (arrowhead).

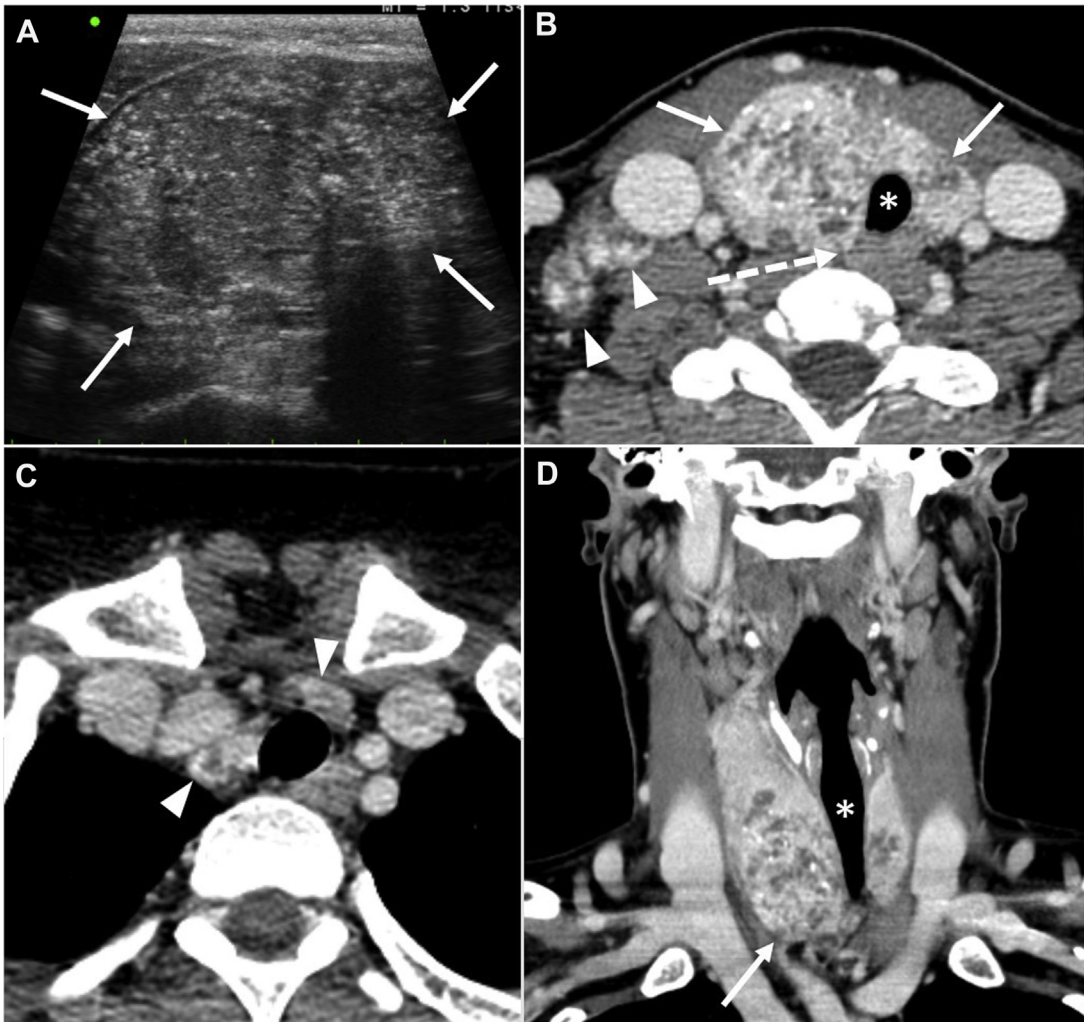


Fig. 12. Papillary thyroid cancer. Transverse gray scale ultrasound image (A) shows a large right thyroid lobe infiltrative hypoechoic solid mass with capsular abutment, contour bulging, and focal loss of echogenic capsule on the left (arrows) with numerous internal echogenic foci compatible with microcalcifications. An axial postcontrast CT scan of the neck (B, C) reveals a heterogeneous tumor with microcalcification centered in the right thyroid lobe with extension across the isthmus to the medial left lobe (arrows). There is more than 180° of tracheal abutment and displacement of the trachea to the left, suspicious for but without frank mucosal tracheal invasion (*). Posterior tumor extension and completely effaced fatty tissue in right tracheoesophageal groove (dashed arrow) is suspicious for tumor invasion of recurrent laryngeal nerve. The tumor abuts the right lateral aspect of the esophagus of less than 180° circumference and without esophageal invasion (dashed arrow). Metastatic lymphadenopathy is seen in the right lower neck (arrowheads in B) and upper mediastinum (arrowheads in C). Coronal postcontrast CT image of the neck (D) shows the craniocaudal dimension of the mass with inferior extension to the sternal notch (arrow) and displacement of the trachea to the left (*).

Papillary Thyroid Carcinoma

PTC is the most common of the differentiated thyroid cancers and has an excellent prognosis and 10-year survival rate of more than 95%.²⁹ In the most recent eighth edition of the AJCC staging system, patients less than 55 years of age are staged as either stage I or II, reflecting the

excellent prognosis, even in the face of nodal metastases and distant metastases.³⁵

Malignant thyroid lesions are more likely to be hypoechoic solid, taller than wide, and lobulated on ultrasound examination and show calcifications (American College of Radiology [ACR]-TIRAD TR5, ATA high suspicion), from 26% to 79%, versus 8% to 39% in benign lesions, with microcalcifications

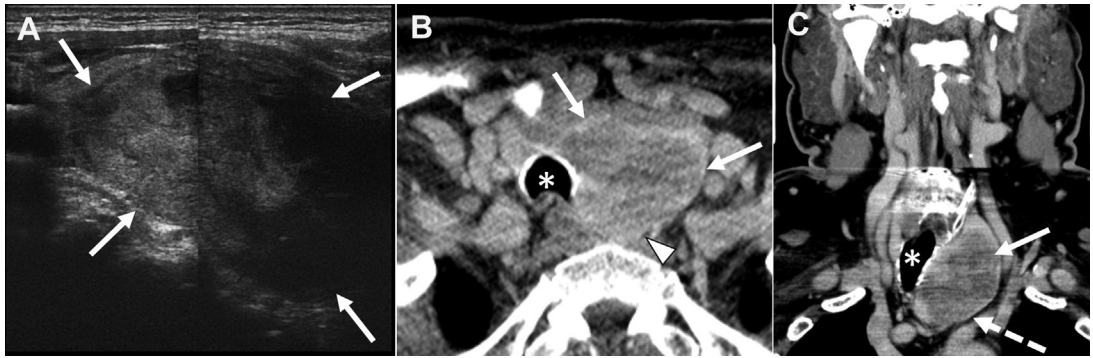


Fig. 13. Follicular variant of PTC with poorly differentiated component. Longitudinal grayscale ultrasound image of the thyroid (A) shows a heterogeneously hypoechoic solid nodule involving most of the left thyroid lobe without internal calcifications (arrows). Axial (B) and coronal (C) postcontrast CT imaging of the neck delineates the mass in the left thyroid lobe (arrows) with inferior extension to the upper mediastinum (dashed arrow) and associated displacement of the trachea to the right (*). Posterior tumor extension and completely effaced fatty tissue in the left tracheoesophageal groove (arrowhead) is suspicious for tumor invasion of the recurrent laryngeal nerve.

Table 1
Comparing the AJCC seventh and eighth editions for differentiated and anaplastic thyroid cancer

Stage	Seventh Edition Description	Seventh Edition 10-y DSS	Eighth Edition Description	Eighth Edition Expected 10-y DSS
Younger patients				
I	Age <45 y All patients without distant metastases regardless of tumor size, lymph node status, or ETE	97%–100%	Age <55 y All patients without distant metastases regardless of tumor size, lymph node status, or ETE	98%–100%
II	Age <45 y Distant metastases	95%–99%	Age <55 y Distant metastases	85%–95%
Older patients				
I	Age ≥45 y ≤2 cm tumor Confined to thyroid	97%–100%	Age ≥55 y ≤4 cm tumor Confined to thyroid	98%–100%
II	Age ≥45 y 2–4 cm tumor Confined to thyroid	97%–100%	Age ≥55 y Tumor >4 cm Or tumor of any size with central or lateral neck lymph nodes or gross ETE into strap muscles	85%–95%
III	Age ≥45 y >4 cm tumor Or minimal ETE or central neck lymph node metastasis	88%–95%	Age ≥55 y Tumor of any size with gross ETE into subcutaneous tissue, larynx, trachea, esophagus, recurrent laryngeal nerve	60%–70%

Adapted from Perrier ND, Brierley JD, Tuttle RM. Differentiated and anaplastic thyroid carcinoma: Major changes in the American Joint Committee on Cancer eighth edition cancer staging manual. *CA Cancer J Clin.* 2018;68(1):55-63. <https://doi.org/10.3322/caac.21439>.

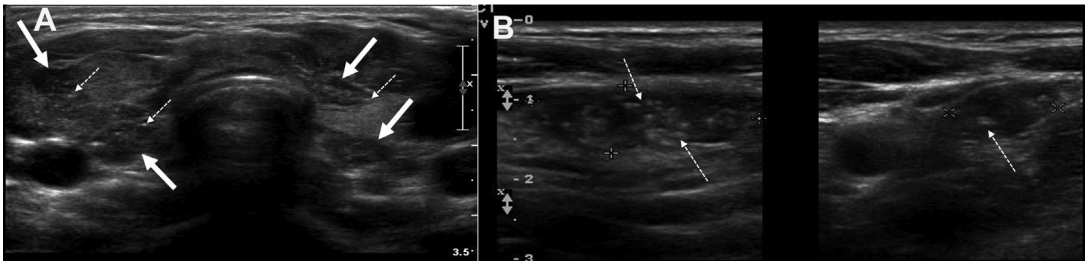


Fig. 14. A 21-year-old woman with an enlarged thyroid on physical examination. A midline transverse grayscale ultrasound image (A) of the thyroid shows enlargement of the gland with multifocal hypoechoic nodules in the bilateral lobes (*white arrows*) with scattered microcalcifications (*dashed arrows*). Dedicated transverse and longitudinal imaging of the right thyroid lobe (B) delineates one such nodule with calipers with hypoechoic echotexture and internal microcalcifications (*dashed arrows*). A biopsy revealed diffuse sclerosing variant of PTC.

more likely found in PTC (see **Figs. 11** and **12**).^{4,5,32} Nodal metastases are a common occurrence in PTC and can be seen in 40% of adults diagnosed with this malignancy.²⁹ Metastatic lymph nodes may be cystic, necrotic, calcified or have internal hemorrhage and are well depicted on ultrasound examination.²⁹ Cross-sectional imaging allows for the careful evaluation of upstaging features including invasion of the trachea, esophagus, strap muscles and tumor extent for surgical planning (see **Figs. 11–13**).

The aggressive variants of PTC typically present with aggressive findings at the time of diagnosis such as ETE and metastasis as well as poorer prognosis compared with the classical PTC. In adults, they include the tall cell variant, columnar cell variant, diffuse sclerosing variant, and follicular variant.^{4,5} The follicular variant typically exhibits features more commonly seen in follicular thyroid carcinoma (FTC), more likely to be isoechoic to hyperechoic, noncalcified, round nodules with regular smooth margins (see **Fig. 13**).^{4,5} The tall cell variant is associated with more aggressive features, such as ETE and nodal metastases, compared with classical and follicular type PTC, and even in cases with just 10% tall cell

composition, this portends a worse prognosis including higher recurrence rates and increased mortality.³⁶ This variant tends to present at older age and with larger tumors compared with classical PTC.³⁷

Diffuse Sclerosing Variant of Papillary Carcinoma

The diffuse sclerosing variant of papillary carcinoma is a rare, aggressive subtype that is generally diagnosed in a younger age group, particularly in female patients.^{38,39} The prevalence is estimated at approximately 0.7% to 6.6% among patients with PTC.³⁹ This variant has a greater propensity for presenting with bilateral lesions, extracapsular extension and nodal metastases.³⁹ On ultrasound examination, the diffuse sclerosing variant of papillary carcinoma is characterized by diffuse enlargement of the thyroid parenchyma with heterogeneous echogenicity and numerous internal hyperechoic foci.³⁸ A large proportion, estimated at up to 83%, of cases show diffuse microcalcifications.³⁸ Additionally, 1 or multiple suspicious masses can be identified in the thyroid gland. These findings closely correlate

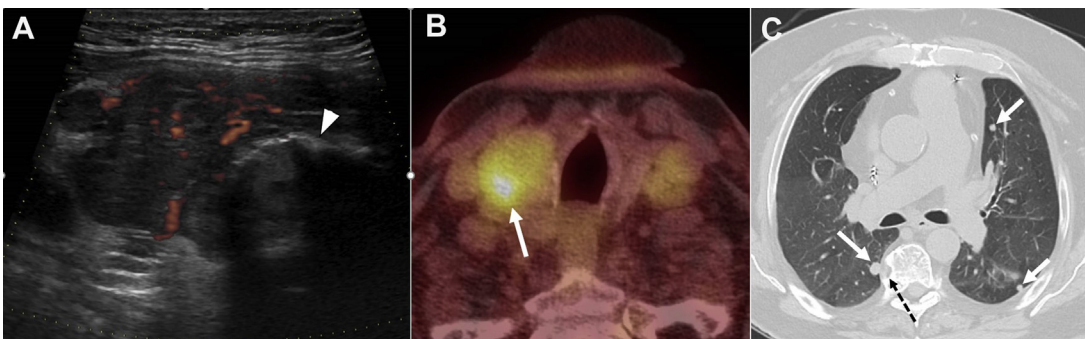


Fig. 15. FTC. Longitudinal grayscale and power Doppler ultrasound images of the thyroid (A) and fused axial PET-CT scan (B) show a lobulated hypoechoic solid hypervascular nodule in the right thyroid lobe with macrocalcification (*arrowhead* on A) and FDG avidity (*arrow* on B). Lung window axial CT imaging of the chest (C) shows multiple pulmonary metastasis (*white arrows*) and vertebral lytic metastasis (*dashed arrow*).

with histopathologic findings of psammoma bodies, widespread fibrosis, and lymphocytic infiltration.³⁸ In summary, this entity should be considered in younger adult patients with enlarged thyroids, scattered microcalcifications and suspicious masses (Fig. 14).³⁸

Follicular Thyroid Carcinoma

FTC is the second most common type of differentiated thyroid cancer after PTC and displays a

more aggressive behavior.⁴⁰ Hematogenous metastatic spread to lung and bones may be seen in up to one-third of patients at presentation, and on pathology vascular invasion may be seen in close to one-half of patients.⁴¹ Spread to cervical lymph nodes is uncommon compared with PTC.²⁹

On ultrasound examination, FTC not only exhibits highly suspicious ultrasound features such as hypoechoic solid, lobulated/irregular margin (ACR-TIRAD TR5, ATA high suspicion), but also typically is more likely to be an isoechoic to

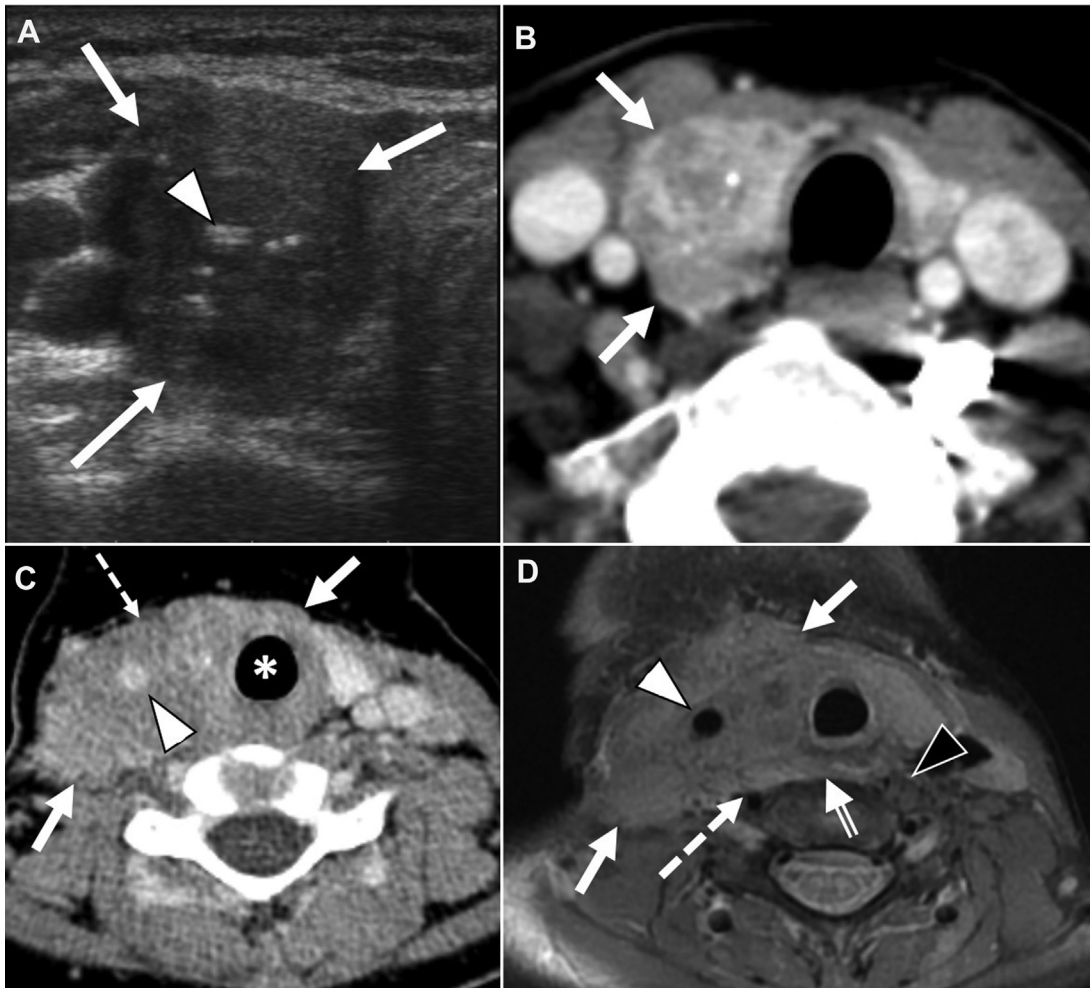


Fig. 16. Spectrum of imaging findings in medullary thyroid cancer. Patient 1 transverse grayscale ultrasound of the right thyroid lobe (A) shows high suspicion features of the nodule (arrows) include markedly hypoechoic, solid, irregular margin, taller than wide and internal calcifications (arrowheads). Axial postcontrast CT image of the neck of the same patient (B) demonstrates a heterogeneous mass with internal calcifications and without ETE (arrows). Patient 2 axial postcontrast CT scan of the neck (C) and T2 fat-saturated axial MR image (D) show an invasive mass in the right thyroid lobe (arrows) with obliteration of the internal jugular vein, and circumferential encasement/invasion of the right common carotid artery (white arrowheads). CT image (C) illustrates circumferential involvement of the trachea by hypodense tumor (*) and invasion of the strap muscles anteriorly (dashed arrow). MR imaging (D) nicely delineates how the mass posteriorly abuts the right vertebral artery (dashed arrow) and ventral vertebral body (double arrow) with invasion of the prevertebral musculature on the right and preservation on the left (black arrowhead).



Fig. 17. Hurthle cell carcinoma. Axial (A, B) and coronal (C) postcontrast CT images of the neck show a large invasive mass centered in the left thyroid lobe with invasion of the strap muscles (*arrows*) as well as mucosal luminal invasion of the trachea (*dashed arrow*). The mass demonstrates caudal extension to the upper mediastinum (*) with gross intraluminal esophageal invasion (*arrowheads*).

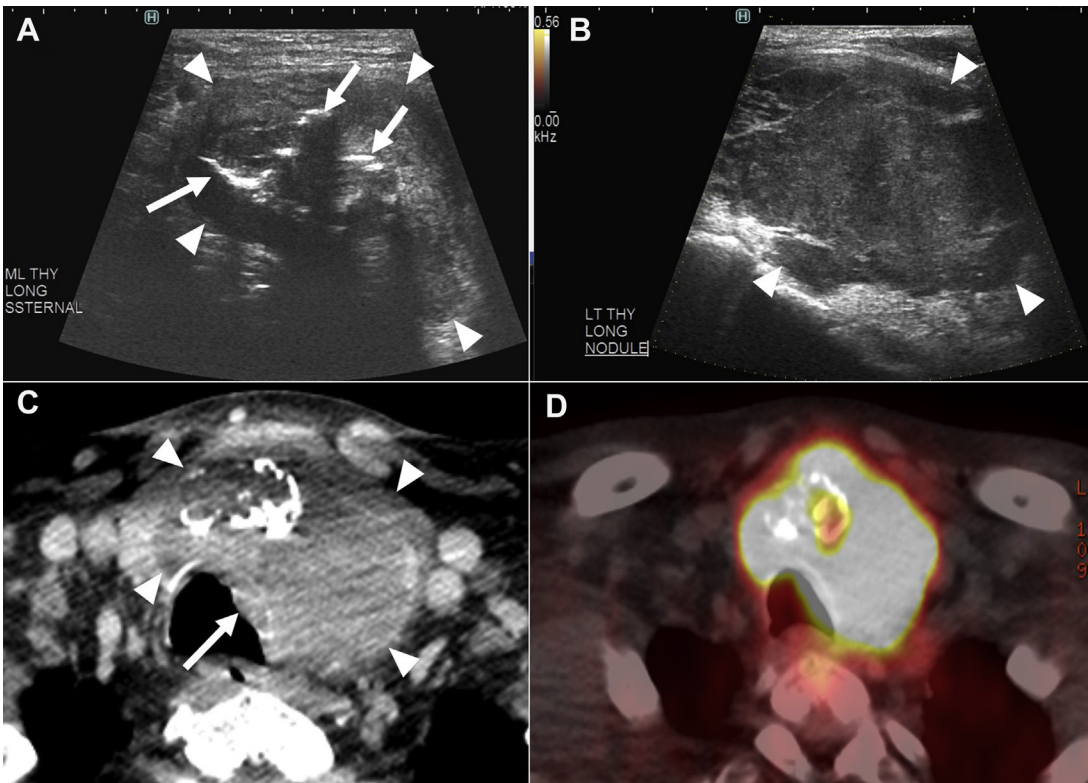


Fig. 18. Anaplastic thyroid cancer in multinodular goiter. Longitudinal grayscale ultrasound image of the isthmus (A) and power Doppler ultrasound image of the left lobe (B) show a hypoechoic mass (*arrowheads*) with calcification (*arrows*). Axial postcontrast CT image (C) and fusion FDG-PET/CT image (D) show the heterogeneous partially calcified FDG avid thyroid mass replacing the entire left thyroid lobe and isthmus (*arrowheads*) and invading the trachea (*arrow*).

hyperechoic, noncalcified, round nodule with regular smooth margins (**Fig. 15**).^{4,5} Microcalcifications are less common in FTC compared with PTC, but the presence of egg shell and macrocalcifications may help to suggest FTC.⁴²

Medullary Thyroid Carcinoma

Medullary thyroid cancer is rare, making up 1% to 2% of all thyroid cancers, but accounts for 13.4% of thyroid-related cancer deaths.⁴³ The majority of cases are sporadic, but approximately 25% cases are associated with *RET* mutations and make up part of the medullary endocrine 2A or 2B neoplasia syndromes.⁴⁴

On ultrasound examination, most medullary thyroid cancers also exhibit the features of high and intermediate ACR TIRAD and ATA suspicion (**Fig. 16**).^{45,46} The presence of microcalcification and the irregular shape of the nodule are significantly associated with metastatic lymph nodes. Medullary thyroid cancer displays aggressive behavior and, at presentation, 35% of patients have ETE or nodal disease and 13% show distant metastatic disease.⁴⁷ Current ATA guidelines recommend evaluation for metastatic disease in patients with calcitonin levels of more than 500 pg/mL.⁴⁸

Multimodality imaging (ultrasound examination, CT scan, MR imaging, and PET/CT scan) is often used to evaluate the full extent of disease from local structural invasion, regional nodal metastasis, to distant lung and bone metastasis. Furthermore, information provided by imaging evaluation aids in determining extent of resectable disease and need for systemic treatment (see **Fig. 16**).³²

Hurthle Cell Carcinoma

Hurthle cell carcinoma is a differentiated tumor demonstrating a more aggressive pattern of behavior compared with PTC. Previously, Hurthle

cell cancer was considered a variant of follicular thyroid cancer; however, recently Hurthle cell cancer has been recognized as a distinct tumor type.⁴⁹ Like FTC, Hurthle cell thyroid cancer has a predilection for hematogenous spread to distant sites such as bone and lungs.⁴⁴

As in other aggressive thyroid cancers, the evaluation of invasive features is important for surgical planning. ETE, including esophageal invasion with luminal disease, requires complete resection of the segment of esophageal tract involvement followed by reconstruction (**Fig. 17**).⁵⁰ When tumor invasion is confined only to the muscularis of the esophagus however, the invaded section can be resected with preservation of the underlying submucosa.⁵⁰

Anaplastic Thyroid Carcinoma

Anaplastic (undifferentiated) carcinoma comprises 2% of primary thyroid carcinomas, most commonly occurs in people over the age of 60 years, and is characterized by locally aggressive, rapidly progressive and invasive tumors that can take over the whole lobe with a 5-month median survival rate and a 1-year survival rate of 20% (**Fig. 18**).¹¹ Therefore, a rapidly enlarging thyroid lobe or gland with airway compromise in adults should raise suspicion for anaplastic carcinoma.

Helpful differentiating features between anaplastic thyroid carcinoma and lymphoma on imaging include the presence of calcifications and necrosis in anaplastic thyroid carcinoma as well as heterogeneous attenuation on CT scans.⁵¹ In contrast, lymphoma shows homogeneous attenuation and lack of calcifications and necrosis.⁵¹ A core biopsy in suspected anaplastic thyroid carcinoma versus lymphoma can aid in initiating prompt diagnosis and treatment.

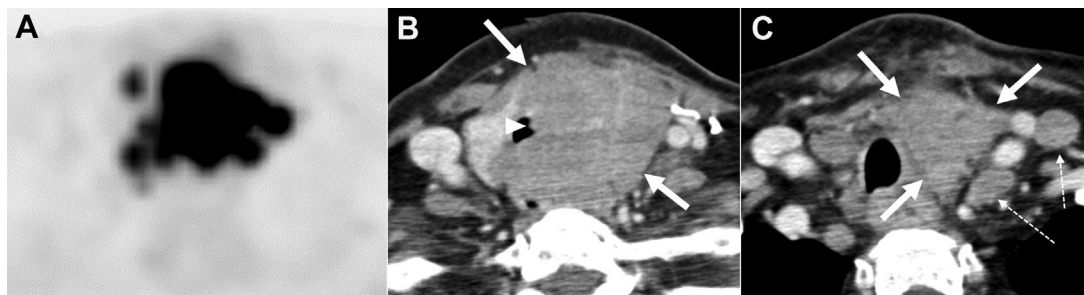


Fig. 19. Thyroid lymphoma. FDG-PET (A) and axial postcontrast CT (B, C) images of a different patient show the FDG avid, noncalcified homogenous soft tissue mass (white arrows) replacing the entire left thyroid lobe, invading the trachea (arrowhead) and associating with solid left lateral neck adenopathy (dashed arrows).

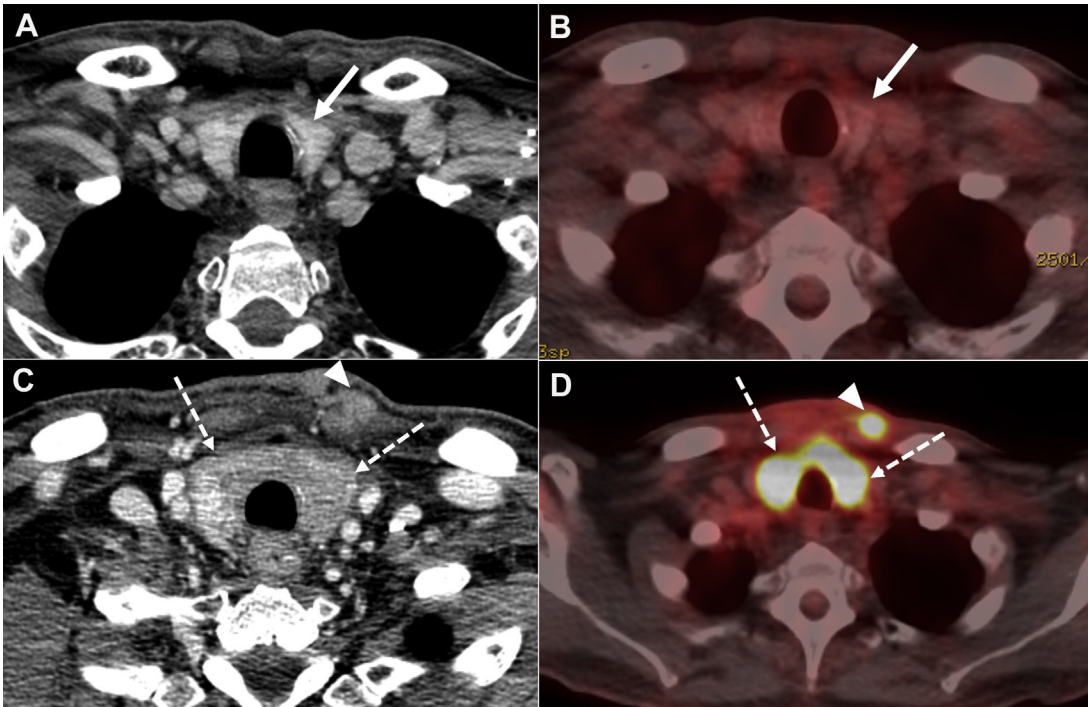


Fig. 20. Thyroid metastasis from squamous cell carcinoma of left base of tongue. Axial postcontrast CT scan of the neck (A) and concurrent axial fused FDG-PET/CT scan at the same level (B) shows a normal-sized thyroid gland with background FDG uptake (*white arrows*). Axial postcontrast CT scan of the neck (C) and concurrent axial fused FDG-PET/CT scan at the same level (D) performed 6 months later reveals interval enlargement and decreased, heterogeneous attenuation of the thyroid gland with markedly increased diffuse tracer uptake (*dashed arrows*) consistent with biopsy-proven metastatic infiltration of the thyroid gland from squamous cell carcinoma. A hypermetabolic subcutaneous nodule in the left upper chest corresponds to an additional metastatic deposit (*arrowhead*).

Thyroid Lymphoma

Thyroid lymphoma makes up 1% to 5% of thyroid malignancies and is characterized by an abnormal proliferation of lymphocytes.¹¹ The most common type of lymphoma to affect the thyroid is extranodal marginal zone B-cell lymphoma, followed by diffuse large B-cell lymphoma. Lymphoma of the thyroid gland generally presents as a single hypoechoic mass on ultrasound (see **Fig. 9**).¹¹ On CT scans, lymphoma of the solid organs often manifests as a solid enhancing mass or diffuse involvement and enlargement and can exhibit local invasiveness. The lymphomatous lymph nodes are generally enlarged and of homogeneous density (see **Fig. 16**). Non-Hodgkin lymphoma of the thyroid is a rare occurrence and generally occurs in elderly women with a prior history of Hashimoto thyroiditis or multinodular goiter. Therefore, in Hashimoto thyroiditis a confluent hypoechoic mass that is, larger than the background 0.1 to 0.6 cm micronodules, should raise suspicion for lymphoma (**Fig. 19**).²⁰

To distinguish between anaplastic thyroid carcinoma or aggressive PTC and thyroid lymphoma, the radiologist must be able to identify classic lymphoma imaging features and recognize the absence of a heterogeneous multinodular thyroid gland, lack of calcifications and absence of cystic lymphadenopathy.⁵²

Thyroid Metastasis

Metastasis may be due to direct invasion or distant dissemination to the thyroid and are considered rare. The most common primary tumors to metastasize to the thyroid include lung, breast and renal cell primaries (**Fig. 20**).²⁷ Ultrasound-guided fine-needle aspiration can be performed for histologic confirmation.⁵³

SUMMARY

Imaging evaluation of the thyroid gland spans a plethora of modalities, including ultrasound examination, cross-sectional studies, and nuclear

medicine techniques. The overlapping of clinical and imaging findings of benign and malignant thyroid disease can make interpretation a complex undertaking. We provide a practical approach to imaging of thyroid disease and highlight the keys to differentiate and diagnose common benign and malignant disease affecting the thyroid gland.

CLINICS CARE POINTS

- Ultrasound examination serves as the most sensitive imaging modality for evaluation of the thyroid parenchyma and for guidance of image-guided biopsies.
- Cross-sectional imaging, including CT scans and MR imaging, serves as an adjunct to assessment of thyroid pathology by providing information on disease extension and characterization of nodal stations not readily evaluated by ultrasound examination.
- The categorization of thyroid disease into diffuse and focal processes aids in narrowing the differential diagnoses.
- Entities that result in diffuse thyroid parenchymal abnormality include a broad spectrum of thyroiditis, with multinodular goiter and malignant infiltration considered within the differential considerations.
- Focal disorders of the thyroid gland include benign and malignant pathology with imaging characteristics that can guide the radiologist to favor certain entities.
- Diffuse sclerosing variant of papillary carcinoma constitutes a rare subtype that is seen in young women portends an unfavorable prognosis and is characterized by diffuse infiltration of the gland with microcalcifications and heterogeneous echogenicity.
- An underlying diagnosis of Hashimoto thyroiditis represents a risk factor for PTL and a questionable risk factor for the development of PTC.

REFERENCES

1. Chung R, Kim D. Imaging of thyroid nodules. *Appl Radiol* 2019;48(1):16-26.
2. Themes UFO. Cross-Sectional Imaging of the Thyroid Gland. *Radiology Key*. 2017. Available at: <https://radiologykey.com/cross-sectional-imaging-of-the-thyroid-gland/>. Accessed September 15, 2020.
3. Allen E, Fingeret A. Anatomy, Head and Neck, Thyroid. In: StatPearls [Internet]. Treasure Island (FL): StatPearls Publishing; 2021. Available at: <http://www.ncbi.nlm.nih.gov/books/NBK470452/>. Accessed September 15, 2020.
4. Haugen BR, Alexander EK, Bible KC, et al. 2015 American Thyroid Association Management Guidelines for Adult Patients with Thyroid Nodules and Differentiated Thyroid Cancer: the American Thyroid Association Guidelines Task Force on Thyroid Nodules and Differentiated Thyroid Cancer. *Thyroid* 2015;26(1):1-133.
5. Amin MB, Edge S, Greene F, et al, editors. *AJCC cancer staging manual*. 8th edition. Cham (Switzerland): Springer International Publishing; 2017. Available at: <https://www.springer.com/gp/book/9783319406176>. Accessed October 15, 2020.
6. Bin Saeedan M, Aljohani IM, Khushaim AO, et al. Thyroid computed tomography imaging: pictorial review of variable pathologies. *Insights Imaging* 2016; 7(4):601-17.
7. Kang T, Kim DW, Lee YJ, et al. Magnetic resonance imaging features of normal thyroid parenchyma and incidental diffuse thyroid disease: a single-center study. *Front Endocrinol* 2018;9. <https://doi.org/10.3389/fendo.2018.00746>.
8. Noda Y, Kanematsu M, Goshima S, et al. MRI of the thyroid for differential diagnosis of benign thyroid nodules and papillary carcinomas. *Am J Roentgenol* 2015;204(3):W332-5.
9. Sakat MS, Sade R, Kilic K, et al. The Use of Dynamic Contrast-Enhanced Perfusion MRI in Differentiating Benign and Malignant Thyroid Nodules. *Indian J Otolaryngol Head Neck Surg* 2019;71(Suppl 1): 706-11.
10. Wang H, Wei R, Liu W, et al. Diagnostic efficacy of multiple MRI parameters in differentiating benign vs. malignant thyroid nodules. *BMC Med Imaging* 2018;18(1):50.
11. Nachiappan AC, Metwalli ZA, Hailey BS, et al. The thyroid: review of imaging features and biopsy techniques with radiologic-pathologic correlation. *RadioGraphics* 2014;34(2):276-93.
12. Sundram F. Clinical use of PET/CT in thyroid cancer diagnosis and management. *Biomed Imaging Interv J* 2006;2(4).
13. Ahuja AT, Ying M. Sonographic evaluation of cervical lymph nodes. *Am J Roentgenol* 2005;184(5):1691-9.
14. Sohn Y-M, Kwak JY, Kim E-K, et al. Diagnostic approach for evaluation of lymph node metastasis from thyroid cancer using ultrasound and fine-needle aspiration biopsy. *Am J Roentgenol* 2010; 194(1):38-43.
15. Sweeney LB, Stewart C, Gaitonde DY. Thyroiditis: an integrated approach. *Am Fam Physician* 2014;90(6): 389-96.
16. Yuen HY, Wong KT, Ahuja AT. Sonography of diffuse thyroid disease. *Australas J Ultrasound Med* 2016; 19(1):13-29.

17. Cappelli C, Pirola I, Martino ED, et al. The role of imaging in Graves' disease: a cost-effectiveness analysis. *Eur J Radiol* 2008. <https://doi.org/10.1016/j.ejrad.2007.03.015>.
18. Intenzo CM, dePapp AE, Jabbour S, et al. Scintigraphic Manifestations of Thyrotoxicosis. *RadioGraphics* 2003;23(4):857–69.
19. Charkes ND, Maurer AH, Siegel JA, et al. MR imaging in thyroid disorders: correlation of signal intensity with Graves disease activity. *Radiology* 1987;164:491–4.
20. Yeh HC, Futterweit W, Gilbert P. Micronodulation: ultrasonographic sign of Hashimoto thyroiditis. *J Ultrasound Med* 1996;15(12):813–9.
21. Virmani V, Hammond I. Sonographic patterns of benign thyroid nodules: verification at our institution. *Am J Roentgenol* 2011;196(4):891–5.
22. Bonavita JA, Mayo J, Babb J, et al. Pattern recognition of benign nodules at ultrasound of the thyroid: which nodules can be left alone? *Am J Roentgenol* 2009;193(1):207–13.
23. Graceffa G, Patrone R, Vieni S, et al. Association between Hashimoto's thyroiditis and papillary thyroid carcinoma: a retrospective analysis of 305 patients. *BMC Endocr Disord* 2019;19(Suppl 1). <https://doi.org/10.1186/s12902-019-0351-x>.
24. Mehta K, Liu C, Raad RA, et al. Thyroid lymphoma: a case report and literature review. *World J Otorhinolaryngol* 2015;5(3):82–9.
25. Moon W-J, Jung SL, Lee JH, et al. Benign and malignant thyroid nodules: US differentiation—multicenter retrospective study. *Radiology* 2008;247(3):762–70.
26. Coskun A, Yildirim M, Erkan N. Substernal goiter: when is a sternotomy required? *Int Surg* 2014;99(4):419–25.
27. Hoang JK, Lee WK, Lee M, et al. US features of thyroid malignancy: pearls and pitfalls. *RadioGraphics* 2007;27(3):847–60.
28. Tran J, Zafereo M. Segmental tracheal resection (nine rings) and reconstruction for carcinoma showing thymus-like differentiation (CASTLE) of the thyroid. *Head Neck* 2019;41(9):3478–81.
29. Hoang JK, Sosa JA, Nguyen XV, et al. Imaging thyroid disease: updates, imaging approach, and management pearls. *Radiol Clin North Am* 2015;53(1):145–61.
30. Kamaya A, Tahvildari AM, Patel BN, et al. Sonographic detection of extracapsular extension in papillary thyroid cancer. *J Ultrasound Med* 2015;34(12):2225–30.
31. Seo YL, Yoon DY, Lim KJ, et al. Locally advanced thyroid cancer: can CT help in prediction of extra-thyroidal invasion to adjacent structures? *AJR Am J Roentgenol* 2010;195(3):W240–4.
32. Traylor KS. Computed Tomography and MR Imaging of Thyroid Disease. *Radiol Clin North Am* 2020;58(6):1059–70.
33. Perrier ND, Brierley JD, Tuttle RM. Differentiated and anaplastic thyroid carcinoma: major changes in the American Joint Committee on Cancer eighth edition cancer staging manual. *CA Cancer J Clin* 2018;68(1):55–63.
34. Tam S, Boonsripitayanon M, Amit M, et al. Survival in differentiated thyroid cancer: comparing the AJCC Cancer Staging Seventh and Eighth Editions. *Thyroid* 2018;28(10):1301–10.
35. Shaha AR, Migliacci JC, Nixon IJ, et al. Stage migration with the new American Joint Committee on Cancer (AJCC) staging system (8th edition) for differentiated thyroid cancer. *Surgery* 2019;165(1):6–11.
36. Vuong HG, Long NP, Anh NH, et al. Papillary thyroid carcinoma with tall cell features is as aggressive as tall cell variant: a meta-analysis. *Endocr Connect* 2018;7(12):R286–93.
37. Cartwright S, Fingeret A. Contemporary evaluation and management of tall cell variant of papillary thyroid carcinoma. *Curr Opin Endocrinol Diabetes Obes* 2020;27(5):351–7.
38. Kwak JY, Kim E-K, Hong SW, et al. Diffuse sclerosing variant of papillary carcinoma of the thyroid: ultrasound features with histopathological correlation. *Clin Radiol* 2007;62(4):382–6.
39. Chereau N, Giudicelli X, Pattou F, et al. Diffuse sclerosing variant of papillary thyroid carcinoma is associated with aggressive histopathological features and a poor outcome: results of a large multicentric study. *J Clin Endocrinol Metab* 2016;101(12):4603–10.
40. Gillanders SL, O'Neill JP. Prognostic markers in well differentiated papillary and follicular thyroid cancer (WDTC). *Eur J Surg Oncol* 2018;44(3):286–96.
41. Grani G, Lamartina L, Durante C, et al. Follicular thyroid cancer and Hürthle cell carcinoma: challenges in diagnosis, treatment, and clinical management. *Lancet Diabetes Endocrinol* 2018;6(6):500–14.
42. Kuo T-C, Wu M-H, Chen K-Y, et al. Ultrasonographic features for differentiating follicular thyroid carcinoma and follicular adenoma. *Asian J Surg* 2020;43(1):339–46.
43. Chen L, Qian K, Guo K, et al. A Novel N Staging System for Predicting Survival in Patients with Medullary Thyroid Cancer. *Ann Surg Oncol* 2019;26(13):4430–8.
44. Cabanillas ME, McFadden DG, Durante C. Thyroid cancer. *Lancet* 2016;388(10061):2783–95.
45. Yun G, Kim YK, Choi SI, et al. Medullary thyroid carcinoma: application of Thyroid Imaging Reporting and Data System (TI-RADS) Classification. *Endocrine* 2018;61(2):285–92.
46. Hahn SY, Shin JH, Oh YL, et al. Ultrasonographic characteristics of medullary thyroid carcinoma according to nodule size: application of the Korean Thyroid Imaging Reporting and Data System and American Thyroid

- Association guidelines. *Acta Radiol* 2020. <https://doi.org/10.1177/0284185120929699>. 284185120929699.
47. Kushchayev SV, Kushchayeva YS, Tella SH, et al. Medullary thyroid carcinoma: an update on imaging. *J Thyroid Res* 2019;2019:1893047.
 48. Wells SA, Asa SL, Dralle H, et al. Revised American Thyroid Association guidelines for the management of medullary thyroid carcinoma. *Thyroid* 2015; 25(6):567–610.
 49. Kakudo K, Bychkov A, Bai Y, et al. The new 4th edition World Health Organization classification for thyroid tumors, Asian perspectives. *Pathol Int* 2018;68. <https://doi.org/10.1111/pin.12737>.
 50. Metere A, Aceti V, Giacomelli L. The surgical management of locally advanced well-differentiated thyroid carcinoma: changes over the years according to the AJCC 8th edition Cancer Staging Manual. *Thyroid Res* 2019;12:10.
 51. Ahmed S, Ghazarian MP, Cabanillas ME, et al. Imaging of anaplastic thyroid carcinoma. *AJNR Am J Neuroradiol* 2018;39(3):547–51.
 52. Johnson SA, Kumar A, Matasar MJ, et al. Imaging for staging and response assessment in lymphoma. *Radiology* 2015;276(2):323–38.
 53. Debnam JM, Kwon M, Fornage BD, et al. Sonographic evaluation of intrathyroid metastases. *J Ultrasound Med* 2017;36(1):69–76.